

*A preprint of*

## **Cellular Systems Biology Profiling Applied to Cellular Models of Disease**

Kenneth A. Giuliano, Daniel R. Premkumar, Christopher J. Strock, Patricia Johnston,  
and D. Lansing Taylor

*To be published in*

Combinatorial Chemistry and High Throughput Screening  
Thematic Issue on In Vitro Imaging (2008)  
Tang, F., and Xu, J., Editors

*Preprint Compliments of*

*Cellumen, Inc.*



*3180 William Pitt Way  
Pittsburgh, PA 15238  
1-866-354-6433*

## **Key Words**

Cellular systems biology; cancer; cellular models of disease; fluorescent protein biosensors; protein-protein interactions; p53; tumor suppressor; high content screening

## **Abstract**

Building cellular models of disease based on the approach of Cellular Systems Biology (CSB)<sup>TM</sup> has the potential to improve the process of creating drugs as part of the continuum from early drug discovery through drug development and clinical trials and diagnostics. This chapter focuses on the application of CSB to early drug discovery. We discuss the integration of protein-protein interaction biosensors with other multiplexed, functional biomarkers as an example in using CSB to optimize the identification of quality lead series compounds.

## **Introduction**

### *Challenge in the pharmaceutical industry*

The goal of the pharmaceutical industry should be to create drugs that exhibit high efficacy, low toxicity and high patient specificity. To reach this goal, there must be changes in the approaches applied to the continuum from early drug discovery, through drug development, and clinical trials and diagnostics. This study addresses the application of Cellular Systems Biology (CSB<sup>TM</sup>) to early drug discovery. CSB can be applied across the continuum from early drug discovery [1] to clinical trials and diagnostics [2].

“Systems biology” is the study of a whole organism viewed as an integrated and interacting network of genes, proteins and metabolic reactions which give rise to life. Thus, the

various disciplines of “omics” (e.g., genomics, proteomics, metabolomics) focus on the parts of a system, while systems biology deals with the functional complexity of the whole. Tissues are collections of specific cell types forming interacting colonies of cells. Although cells and tissues are less complex than a complete organism, they possess significant functional complexity allowing a detailed understanding of many aspects affecting a whole organism, such as the cellular basis of disease, treatment efficacy and potential toxicity of treatments.

“Cellular models of disease” are comprised of cells associated with a diseased state wherein the cells are either isolated from a diseased tissue or the cells are manipulated to exhibit one or more disease phenotypes [3]. A cellular systemic approach to developing cellular models of disease involves the integration of multiplexed fluorescent biomarkers coupled with searchable databases and automated informatics to reduce the complex data sets to values that can be used in making decisions.

CSB uses panels of biomarker measurements to investigate the integrated and interacting networks of genes, proteins, and metabolites that are responsible for normal and diseased cell functions [3-5]. “Biomarkers” in our context, are cellular constituents, activities, or both (e.g., protein or other macromolecules, organelles, ions, metabolites, etc.) that can be specifically labeled and measured with fluorescence based reagents (e.g., fluorescently labeled antibodies, fluorescent protein biosensors, fluorescent physiological indicators, etc.).

A “feature” is an image-based measurement or series of measurements of a particular biomarker that can include, but not limited to, morphometric, intensity, localization, and ratios or differences, that can indicate a biological function or activity. Biological functions indicated by biomarkers include, but are not limited to: protein posttranslational modifications such as phosphorylation, proteolytic cleavage, methylation, myristoylation, and attachment of

carbohydrates; translocations of ions, metabolites, and macromolecules between compartments within or between cells; changes in the structure and activity of organelles; and alterations in the expression levels of macromolecules such as coding and non-coding RNAs and proteins, morphology, and state of differentiation.. A single biomarker can provide a read-out of more than one feature. For example, Hoechst dye can be used to detect DNA (e.g., a biomarker), and a number of features of the cells (e.g., nucleus size, cell cycle stage, number of nuclei, presence of apoptotic nuclei, etc.) can be identified by the DNA detected with the Hoechst dye.

A “CSB profile” is a systemic characterization of the interactions, relationships, or state of the constituents of cells as indicated by usually > 6 biomarkers that give rise to the CSB features (usually > 10) that are used to construct the profile. The interrelationships within a cellular systems biology profile are defined, for example, either arithmetically (e.g., ratios, sums, or differences between cellular systems biology feature values) or statistically (e.g., hierarchical clustering methods or principal component analyses of combinations of cellular systems biology feature values).

CSB builds on the tools of High Content Screening (HCS), which was introduced more than 10 years ago to combine some of the efficiencies of HTS with biological context of the intact cell. HCS makes it possible to determine the effect of experimental compounds on target molecules, usually proteins, within the context of the living cell. However, the focus of HCS continues to be on individual target protein activities and falls short of elucidating cellular activity as the function of a system [4, 6]. CSB aims to profile the response of the cellular “system” to compounds designed to impact specific target(s) in order to identify both efficacy and potentially harmful off-target effects. Therefore, CSB provides more highly qualified leads on more highly validated targets.

CSB profiling is a key component of cellular models of disease that can find applications within several steps of the drug discovery process. Furthermore, incorporation of cellular models of disease into the drug discovery process has the potential to improve efficacy and decrease toxicity of leads and clinical candidates.

*The tools of CSB are used to manipulate and measure cellular models of disease*

To take full advantage of cellular models of disease at the systems level requires an understanding of the activities of organelles, metabolites, protein-protein interactions, protein modifications, protein translocation, protein conformational changes, lipids, nucleic acids, and carbohydrates as well as feedback and feedforward mechanisms that regulate cellular systems [7]. Reagents that couple specific molecular manipulations with CSB profiling in cellular models of disease have been recently reviewed [8] and a specific example of using gene switches to manipulate protein levels has been discussed [4]. Fluorescent protein biosensors of protein-protein interactions are one of the most powerful reagent classes to be integrated into cellular models of disease. The optimal characteristics of protein-protein interaction biosensors (PPIBs) have been recently discussed [7]. An ideal PPIB is specific, sensitive, reversible and does not alter normal cell functions [6].

To demonstrate our approach to building a relevant cellular model of cancer, we developed a CSB profile where one biomarker feature measurement is a key protein-protein interaction involved in the regulation of the DNA damage response as well as apoptosis, the p53-HDM2 interaction. We first demonstrate how we evaluated an adenoviral-based gene delivery system for its potential to perturb multiple cellular functions before using it to deliver a PPIB of the p53-HDM2 protein-protein interaction into an osteosarcoma model. Next, we used a similar

approach to maximize the population of cells that express biosensing levels of the p53-HDM2 PPIB while minimizing the population of cells expressing biosensor levels that alter cell function. Finally, we integrated p53-HDM2 PPIB measurements into a CSB profile consisting of 12 biomarker activity measurements within the same population of human tumor cells. The profile made it possible to put biosensor activity measurements in the context of other cellular systems responses including those directly related to p53 activation such as the induction of ATM kinase and DNA repair response activities as well as changes in nuclear morphology and DNA content. Furthermore, we also profiled related cellular systems responses involved in the regulation of the actin and microtubule cytoskeleton, stress kinase activation, cell adhesion, immune and inflammation response, and organelle activity regulation. This systems approach enabled us to not only screen for compounds that disrupted the p53-HDM2 interaction, but to show that active compounds disrupted the p53-HDM2 interaction by manipulating distinct cellular systems and potentially involved off-target effects not desired.

## **Materials and Methods**

### *Reagents*

The histone deacetylase inhibitor MS-275 and the cdc2 kinase inhibitor RO-3306 were purchased from Axxora, LLC (San Diego, CA). The rest of the compounds listed in Table 1 plus the Hoechst 33342 and 37% formaldehyde were from Sigma Chemical Company (St. Louis, MO). Hyclone brand cell culture medium, fetal bovine serum, trypsin, and HBSS were from Thermo Fisher (Waltham, MA). Labeled secondary antibodies were from Jackson ImmunoResearch Laboratories, Inc. (West Grove, PA).

### *Cell culture and drug treatment*

Human A549 lung carcinoma cells (CCL-195) were obtained from the American Type Culture Collection (ATCC; Manassas, VA). Cells were cultured in complete McCoy's growth medium plus 10% fetal bovine serum and penicillin-streptomycin. For drug treatment, cells infected with adenoviruses expressing the two p53-HDM2 PPIB components (see below) were plated at a density of 5000 cells per well (40  $\mu$ l) in 384-well microplates (Falcon #3962; Thermo Fisher) that were coated with collagen I. Cells were exposed to drugs 24 h after plating. Concentrated stocks of all drugs were diluted into solutions of HBSS plus 10% fetal bovine serum and added to the microplates (10  $\mu$ l per well) using an automated liquid handling system (Biomek® 2000; Beckman-Coulter, Inc., Fullerton, CA).

### *p53-HDM2 PPIB construction and delivery into cells*

The basic construction of the p53-HDM2 PPIB has been described in detail [7]. We used an adenoviral-based delivery system to express the biosensor in A549 cells. Recombinant adenoviruses for each component of the p53-HDM2 PPIB were constructed by inserting the expression cassettes of each of the biosensor components into the adenovirus genome in the E1 deletion site of the replication defective adenovirus genome. This was achieved using the recombinant adenovirus production method developed by Mizuguchi and Kay [9]. In short, the p53 and hDM2 biosensor expression cassettes were inserted into a shuttle plasmid which was used to shuttle the expression cassette into the adenovirus genome. The highly specific endonucleases, I-Ceu I and PI-Sce I, were used to digest the shuttle plasmid and the adenoviral plasmid for in vitro ligation of the expression cassette to insert each of the two biosensor components into separate adenoviral plasmids. These were then screened for the recombinant

adenovirus. Adenoviruses expressing each component of the biosensor were then produced in HEK-293 cells and stored at -80 C until needed.

To produce large populations of A549 cells expressing the two-component p53-HDM2 PPIB,  $3 \times 10^6$  cells were infected with both components of the biosensor at the levels described in the Results section for 1 h at 37 C in a total volume of 200  $\mu$ l and then transferred to 384-well microplates as described above before treatment with compounds.

#### *Immunofluorescence labeling and HCS*

At the end of an experiment, cells were fixed, permeabilized, and the biomarkers were labeled with the immunoreagents listed in Table 2 using the methods described elsewhere [10, 11]. Likewise, HCS of prepared microplates was performed as described [10, 11].

#### *Statistical analysis and data visualization*

To determine the significance of the cellular population changes induced by treatment with drug molecules, we used a Kolmogorov-Smirnov (KS) goodness of fit analysis (KS value) [10, 11]. Two-dimensional contour plots or Distribution maps of the CSB profiling data were used to project three-dimensional surface plots onto a two-dimensional plane [10]. Blue shades encoded the lowest population densities while shades of yellow and red encoded the highest population densities. Furthermore, multiple Distribution maps were easily arrayed for the simultaneous visualization of multiplexed HCS data sets. Cell maps were used to decipher connections between biomarkers in the same populations of cells and the effects drugs have on these relationships [10]. Like Distribution maps, Cell maps are plots of cell density values that

are color encoded. Cell maps were used to simultaneously plot the cellular responses of two biomarkers to facilitate the visualization of relationships between biomarker responses

## **Results**

### *The adenoviral gene delivery system had minimal effects on multiple cell biomarkers*

We infected A549 cells with an adenovirus encoding a fluorescent protein to define the optimal levels that produced good signals from the biosensor without altering cell function. Fig. (1) shows that expression of a fluorescent protein at multiple levels did not perturb multiple functional biomarkers of several key cell indicators when measured by changes in nuclear size, chromatin condensation, or cell cycle regulation.

### *Optimizing the expression level of the p53-HDM2 PPIB produced large populations of qualified biosensing cells*

After demonstrating that the adenoviral gene delivery system was minimally perturbing to cell function, we measured the effects of the p53-HDM2 PPIB on the same biomarkers. A549 cells were infected with the two-component p53-HDM2 PPIB expression vector system at a total MOI of 1.03 with a p53:HDM2 adenovirus concentration ratio (IFU/ml) of 34:1.

After incubation for 24 h, the expression levels of the HDM2 PPIB component in untreated cells were divided into 15 bins, each containing an equal number of cells. The top set of distribution maps in Fig. (2) show the expression level of the HDM2 PPIB component in each of the bins. The other distribution maps showed the effects of biosensor expression on cell activity. These distribution maps show that 14 out of the 15 expression levels contained biosensor expression levels qualified to reliably measure effects of compounds on the p53-

HDM2 protein-protein interaction because they minimally perturbed key cell activities. Thus, selecting the expression level of the PPIB enabled us to reliably incorporate the biosensor into a CSB profile that was used to build functional relationships between biomarker activities and the activities of compounds that modulated these relationships.

*Automated cluster analysis of CSB profiling data facilitated a mechanistic understanding of p53-HDM2 interaction modulating compounds*

Coupling the measurement of 13 biomarker responses to treatments with 14 compounds at 12 concentrations each produced an extensive CSB profile of over 2 million measurements that could not be readily interpreted manually. Fig. (3) shows that automated hierarchical clustering of the p53-HDM2 PPIB activity data could be used to quickly pinpoint p53-HDM2 interaction modulating compounds. Furthermore, the CSB profiling data, which were collected at the same time as the biosensor activity measurements, enabled us to compare the effects of the p53-HDM2 interaction modulating compounds on multiple cellular systems in the same population of cells. For example, the set of 14 compounds that were profiled had a wide range of known activities (Table 1), but a cluster of three exhibited consistently high p53-HDM2 protein interaction disrupting activity. Nutlin-3, camptothecin, and anisomycin formed a closely related activity cluster as defined by their common p53-HDM2 PPIB activity (Fig. (3), green boxes). When the CSB profiling data for the other biomarker activities were also clustered according to the p53-HDM2 PPIB activity results, further insight into the mechanism of action of each of the compounds was facilitated: 1) Nutlin-3 showed the greatest modulation of the p53-HDM2 interaction over the 2 h time course out of the three most active compounds. The clustered heat maps indicate that nutlin-3 did not consistently alter other biomarker activities in the CSB

profile over the two hour treatment time period. However, it was determined that nutlin-3 caused significant toxicity at treatment levels  $> 50 \mu\text{M}$  where it induced  $> 70\%$  cell loss (data not shown). ; 2) Camptothecin, which is known to induce p53 activity over a time course of 24 h [11], significantly (*e.g.*, KS value  $> 0.2$ ) [10, 11] modulated the phosphorylation levels of ATM kinase substrates, one of which is p53, in addition to disrupting the p53-HDM2 interaction whereas nutlin-3 and anisomycin were not as active (Fig. (3), black arrow); and 3) Anisomycin on the other hand induced a significant and predictable change in ATF-2 phosphorylation levels at several concentrations (Fig. (3), red arrow).

Automated analysis of the large CSB profiling database therefore provided initial mechanistic information on the compounds that had the greatest effect on the target of interest, the p53-HDM2 protein-protein interaction. Nevertheless, clustering the profiling data on other biomarker features has the potential to reveal other cellular systems relationships and mechanistic profiles of the other compounds that were assayed.

*CSB profiling showed that p53-HDM2 protein-protein interaction modulators can act through distinct cellular systems*

The compound set we profiled was comprised of relatively well characterized entities (Table 1). Nonetheless, using a novel biosensor of the p53-HDM2 interaction it was demonstrated that camptothecin and anisomycin disrupted the p53-HDM2 interaction over the moderately short time course of 2 h, an activity that we would have predicted for only one member of the compound set, nutlin-3. Because the PPIB measurement was integrated within a CSB profile, we were able to drill down into the database to further investigate these unpredicted results. Fig. (4) shows more detailed information from the CSB profile that differentiates the

mechanisms by which the three compounds disrupt the p53-HDM2 interaction. The cell population responses showed that nutlin-3 was the most active of the three compounds in disrupting the p53-HDM2 interaction. However, nutlin-3 did not induce the activation of ATM kinase activity as much as camptothecin. This result is consistent with the finding that nutlin-3 treatment of cells does not induce the phosphorylation of p53 at the ATM kinase specific phosphorylation site [12]. Furthermore, nutlin-3 did not induce any activation of the transcription factor ATF-2, while anisomycin did induce ATF-2 activation. While these results are consistent with the three compounds acting via different mechanisms, CSB profiling data showing the relationships between functional biomarker activities in the same cell populations provide even more compelling information on the mechanism of each of the compounds.

Cell Maps were used to demonstrate the relationships between two CSB profiling biomarkers in the same cell population (Fig. (5)). The first column of Cell Maps show that nutlin-3 induced a relatively homogeneous disruption of the p53-HDM2 interaction as well as a small decrease in the activity of ATM kinase in the same cells (Fig. (5), white arrows). In contrast, both camptothecin and anisomycin induced a more heterogeneous disruption of the p53-HDM2 interaction than did nutlin-3. Furthermore, the second column of Cell Maps show that camptothecin induced ATM kinase activity in the same cell population that exhibited disruption of the p53-HDM2 interaction (Fig. (5), green arrows), while the third column of Cell Maps shows that the p53-HDM2 disrupting activity of anisomycin was not accompanied by ATM kinase activation in the same cell population.

That camptothecin induced a significant disruption of the p53-HDM2 interaction in those cells where ATM kinase substrate phosphorylation levels were also elevated is consistent with a mechanism where camptothecin activated ATM kinase which, in turn, phosphorylated many

substrates, including serine 15 of p53. Phosphorylation of p53 by ATM kinase is correlated with the activation of p53 in cells, but may not be directly related to disruption of the p53-HDM2 interaction through phosphorylation at serine 15 [13]. Nevertheless, CSB profiling was able to build a relationship between the activation of ATM kinase and the disruption of the p53-HDM2 PPIB in the same cells. Incidentally, the p53-HDM2 PPIB contains the ATM kinase phosphorylation site on the p53-based component. However, no concentrated nucleolar labeling of the ATM substrate phosphorylation specific antibody was detected suggesting that the anchored p53-component of the PPIB was not accessible for ATM phosphorylation.

In contrast, the disruption of the p53-HDM2 interaction without a concomitant increase in ATM kinase substrate phosphorylation induced by nutlin-3 treatment was consistent with a direct disruption of a specific protein-protein interaction. In fact, nutlin-3 was designed to directly target the interaction site between p53 and HDM2 [14] and has been found to not induce the phosphorylation of p53 on 6 key serine residues, including the site specific phosphorylated by ATM kinase [15].

Finally, anisomycin showed p53-HDM2 interaction disrupting activity without increasing or decreasing the ATM kinase phosphorylation levels in the same cell population, but anisomycin significantly increased the activity of the transcription factor ATF-2 whereas nutlin-3 did not. This suggests that anisomycin may also disrupt the p53-HDM2 interaction indirectly, perhaps through its activation of the c-jun stress kinase pathway, the kinase cascade known to result in ATF-2 phosphorylation.

## **Discussion**

*There is a need for cellular models of disease in the drug discovery process*

Until recently, the focus in drug discovery and basic biomedical research has been on simplifying the complexity of the living human organism to individual genes, single metabolic pathways, single proteins, and one potential modulating molecule such as a small chemical compound or bioproducts to regulate complex functions. This one gene, one protein, one external modulating treatment concept dominated the drug discovery process and much of basic biomedical research for the last 15 years. This paradigm grew out of the promise of the human genome project and the theory that identifying all protein coding genes would lead to much more rapid discovery of cures for human disease [16-18].

Unfortunately, this reductionist approach to drug discovery has not delivered the promised efficiencies. Multiple genes, including both protein coding and non-coding genes, regulate most cellular processes [19-22], and proteins are part of complex, interacting pathways with extensive compensatory capacities. Therefore, even when a single, small molecule or bioproduct has a specificity for binding to a single protein, the impact on cellular and therefore, tissue and organ function is much more complex than expected [23]. In addition, absolute specificity of small molecules and biologics are rarely demonstrated and “off target” effects must be understood for both efficacy and potential toxicity [24, 25]. Finally, most diseases are multifactorial where the disease phenotype arises from the dysregulation of multiple genes, pathways and proteins [26-29].

Thus, a need exists to provide methods for producing, analyzing and profiling the multifactorial processes of disease in order to more fully understand the systemic and complex interaction of disease-based cellular biology systems and to elucidate appropriate treatments. CSB profiling is fundamental to creating cellular models of disease because it harnesses the higher throughput capacity of automated microscopy technologies while avoiding the expense

and potential confounding species related problems associated with traditional organism-based systems biology [4]. CSB profiles are therefore a systemic characterization in a context defined as the study of the living cell, the basic “unit of life”; an integrated and interacting network of genes, proteins and myriad metabolic reactions that give rise to function [3, 6, 10].

*Protein-protein interaction biosensors are valuable functional biomarkers of this class of target, especially when integrated into a cellular model of disease*

Guidelines for the design and validation of fluorescent protein biosensors have been available for more than 10 years and have been recently reviewed [7, 8]. Here, we applied these key concepts to show how PPIBs can be integrated into cellular models of disease.

We previously reported on the construction and validation of a PPIB for the p53-HDM2 interaction that was delivered to cells using a non-scalable expression vector transfection-based approach [7]. As demonstrated here for the first time, the positional biosensor of the p53-HDM2 interaction can be successfully expressed in large populations of cells to perform screening assays with high capacity using an adenoviral-based delivery system. Furthermore, we made multiplexed measurements to define assay conditions where neither the biosensor delivery system nor the biosensor itself significantly perturbed normal cell function.

We incorporated the p53-HDM2 interaction biosensor measurement into a CSB profile that provided 12 other biomarker activities of cellular systems important in defining a cellular model of cancer (Table 2). For example, functional biomarkers of kinase activities, the DNA damage response, and nuclear morphology and chromatin regulation, all of which are closely coupled to the p53 signaling system, were incorporated into the CSB profile. In addition, other biomarkers of cellular systems involved in cancer as a disease process such as cytoskeletal

regulation, organelle function, and immune system responsiveness, were integrated into the same CSB profile.

*Cellular models of disease provide a method for profiling the treatment of a disease state with leads and clinical candidates at critical decision points in the drug discovery process*

We profiled 14 compounds with a wide range of known activities (Table 1) using the CSB-based cellular model of disease. The automated classification analysis of the large profiling database was found to partition at least three active disruptors of the p53-HDM2 interaction into a small cluster separate from the other compound activities. However, if we consider the p53-HDM2 interaction as the primary target of the screen, the larger CSB profiles from this small test library of compounds clearly showed that the three p53-HDM2 interaction inhibitors all had serious potential problems. Nutlin-3 exhibited toxicity, while anisomycin and camptothecin displayed potentially serious off-target effects, even after only 2 h of treatment.

Nutlin-3, a compound designed to directly disrupt the p53-HDM2 interaction [14], provided the expected PPIB activity and became the most active member of this active cluster. That nutlin-3 exhibited specific p53-HDM2 disrupting activity as well as an early indicator of cytotoxicity (*e.g.*, induction of cell loss), but did not modulate the other biomarkers we profiled, prompted us to further investigate the activity of nutlin-3 with CSB approach designed specifically for toxicity profiling [1]. We obtained pre-clinical safety data for nutlin-3 over multiple time courses (60 min, 24 h, and 72 h) with an 11 biomarker feature set using a CellCiphr™ profile based on human hepatocellular carcinoma cells [1]. The preclinical safety data showed that nutlin-3 was relatively inactive against cytotoxicity biomarkers other than cell loss at treatment concentrations up to 250  $\mu$ M over a time course of 60 min, a time course similar to that used in this study.

However, toxicity profiling of nutlin-3 over a 24 h treatment showed that the drug induced not only cell loss, but also caused a decrease in nuclear size and induced a p53 activation response. Thus, nutlin-3 can induce cytotoxicity over a relatively short time course without modulating biomarkers for stress kinase activation, microtubule cytoskeletal regulation, the DNA damage response, and mitochondrial function. Over a longer time course though, nutlin-3 does induce p53 activation [14].

Somewhat unexpectedly, camptothecin and anisomycin also induced significant PPIB activity, which resulted in them being included in the active cluster along with nutlin-3. That the p53-HDM2 PPIB biomarker measurements were integrated into the CSB profile enabled us to drill further down into the cellular systems that nutlin-3, camptothecin, and anisomycin modulated in addition to their p53-HDM2 interaction disrupting activity.

The value of applying CSB profiling to cellular models of disease in early drug discovery is to identify potential lead series for a selected primary target (*e.g.*, p53-HDM2 interaction) in the context of potentially serious off-target effects due to the cellular systems response. It is proposed that the lead series selected from this step be further profiled in the CellCiphr Cytotoxicity panel(s) to better prioritize the lead series, saving time and money in the process [1].

## **Summary**

By coupling automated data analysis and tools to visualize the functional responses of cell populations, we were able to conclude that nutlin-3, camptothecin, and anisomycin disrupted the p53-HDM2 interaction via perturbation of distinct cellular regulatory systems. The example discussed in this chapter demonstrates how a particular target (*e.g.*, p53-HDM2 interaction) is

analyzed with a cellular systems biology response profile that can optimize the selectivity of lead compounds based on both efficacy and potentially serious off-target effects. The selection of a lead series priority can be subsequently determined by applying CSB to cytotoxicity profiling [1]. Thus, cellular models of disease are part of the continuum of CSB approaches that are applied from early drug discovery through drug development and into clinical trials and diagnostics.

### **Conflict of Interest**

All authors are full time employees of Cellumen, Inc., a company that creates cellular systems biology products and services.

### **Acknowledgments**

Funding for this project was provided in part by the Pennsylvania Department of Health. Positional biosensor patent portfolio licensed from Cellomics, fluorescent proteins licensed from Evrogen and adenoviral delivery system licensed from Stanford University. Cellumen patents pending.

Table 1. Compound set used to demonstrate CSB profiling with example activity biomarkers

<b>Compound</b>	<b>Abbreviation</b>	<b>Concentration Range</b>	<b>Example Compound Activity Biomarkers</b>
Anisomycin	ANIS	5 nM – 10 $\mu$ M	Stress kinase activation; protein synthesis inhibition
Camptothecin	CMPT	24 nM – 50 $\mu$ M	Topoisomerase I inhibition; induction of DNA damage; activation of p53; and apoptosis
Etoposide	ETOP	24 nM – 50 $\mu$ M	Topoisomerase II inhibition; induction of DNA damage; activation of p53; and apoptosis
MS-275	M275	24 nM – 50 $\mu$ M	Histone deacetylase inhibition; induction of reactive oxygen species
Nutlin-3	NUT3	49 nM – 100 $\mu$ M	p53-HDM2 interaction inhibition; modulation of cell cycle regulation
Paclitaxel	PCTX	2.4 nM – 5 $\mu$ M	Microtubule stabilization; modulation of mitosis regulation
Trichostatin A	TRSA	24 nM – 50 $\mu$ M	Histone deacetylase inhibition; modulation of cell cycle regulation
Tumor Necrosis Factor - $\alpha$	TNFA	0.1 ng/ml - 200 ng/ml	<i>NF-<math>\kappa</math>B</i> transcription factor activation; induction of apoptosis
RO-3306	R336	24 nM – 50 $\mu$ M	Cdc2 kinase inhibition; modulation of mitosis regulation

Roscovitine	ROSC	24 nM – 50 $\mu$ M	Inhibition of cyclin dependent protein kinase 5 (CDK5); induction of apoptosis
U0126	U012	24 nM – 50 $\mu$ M	Selective inhibition of MEK1 and MEK2 activity; modulation of anchorage-dependent growth
Vinblastine	VNBL	0.49 nM – 1 $\mu$ M	Microtubule destabilization; modulation of mitosis regulation
2-Methoxyestradiol	METE	49 nM – 100 $\mu$ M	Modulation of microtubule stability; modulation of angiogenesis
5-Fluorouracil	FLUR	49 nM – 100 $\mu$ M	Thymidylate synthase inhibition; modulation of cell cycle S-phase regulation; and activation of p53

Table 2. CSB profile biomarker activities, the primary antibody reagents, and their associated feature measurements

<b>Biomarker Activity</b>	<b>Primary Antibody Reagent and Source</b>	<b>CSB Feature Measurement</b>
p53-HDM2 interaction	-	p53-HDM2 PPIB activity
ATM kinase activity	Rabbit anti-ATM substrate motif (Cellular Signaling Technologies, Danvers, MA)	ATM(Ser/Thr) substrate phosphorylation level
Stress kinase activation	Rabbit anti-phospho-ATF-2 (T71) (Cellular Signaling Technologies)	ATF-2(Thr71) phosphorylation level
DNA repair response	Mouse anti-APE (Affinity Bio Reagents, Golden, CO)	Apurinic/Apyrimidinic Endonuclease 1 (APE) nuclear expression level
Mitochondrial mass change	Mouse anti-mtHSP70 (Affinity Bio Reagents)	Total mitochondrial expression level of mtHSP70 protein
Microtubule cytoskeleton stability	Mouse anti- $\alpha$ -tubulin (Sigma Chemical Company, St. Louis, MO)	Total level of $\alpha$ -tubulin after detergent extraction
14-3-3 cytoskeleton associated protein stability	Rabbit anti-14-3-3 (Sigma Chemical Company)	Total level of 14-3-3 protein after detergent extraction
Actin cytoskeleton	Rabbit anti-cofilin (Sigma	Total level of actin binding protein

assembly state regulation	Chemical Company)	cofilin in nuclear compartment
Cell adhesion regulation	Rabbit anti-phospho-FAK (Sigma Chemical Company)	Total level of cytoplasmic focal adhesion kinase phosphorylation (pFAK)
Inflammatory and immune response regulation	Rabbit anti-NF- $\kappa$ B (p65) (Santa Cruz Biotechnology, Santa Cruz, CA)	NF- $\kappa$ B transcription factor cytoplasm to nuclear translocation
Nuclear morphology and chromatin regulation	-	Multiple measurements of nuclear shape and size as well as chromatin condensation

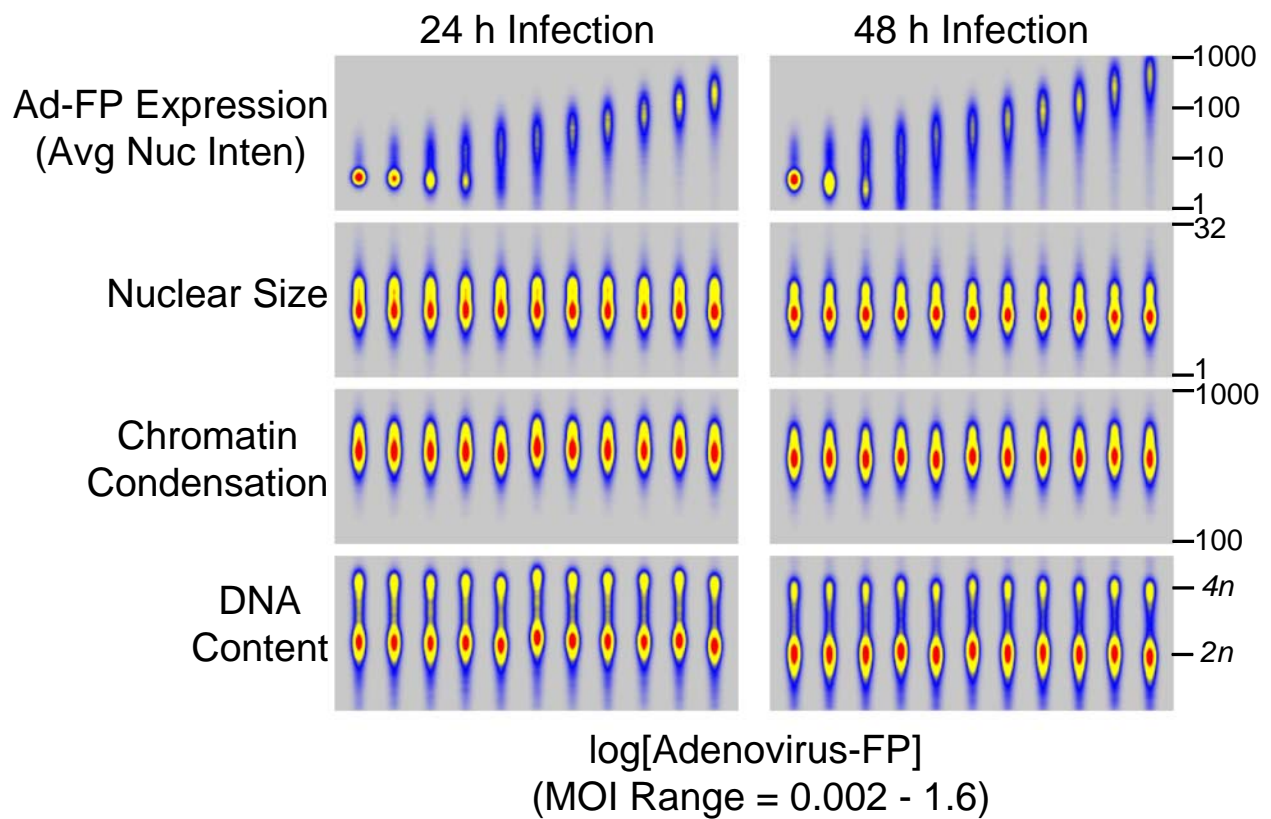


Figure 1. An adenoviral gene delivery system had minimal effects on cell cycle and nuclear morphological regulation in short term cell-based assays. A549 cells were infected with multiple levels of an adenovirus gene delivery system encoding a fluorescent protein. Distribution maps show multiple cell population responses (Y-axis) at each level of adenoviral infection (X-axis). Maximal fluorescent protein levels were within an order of magnitude of each other at both 24 and 48 h. Biomarkers of cell activity including nuclear size, chromatin condensation, and DNA content showed no change across the entire range of adenoviral infection levels, consistent with the adenoviral gene delivery and the fluorescent protein cargo it encoded as being minimally perturbing.

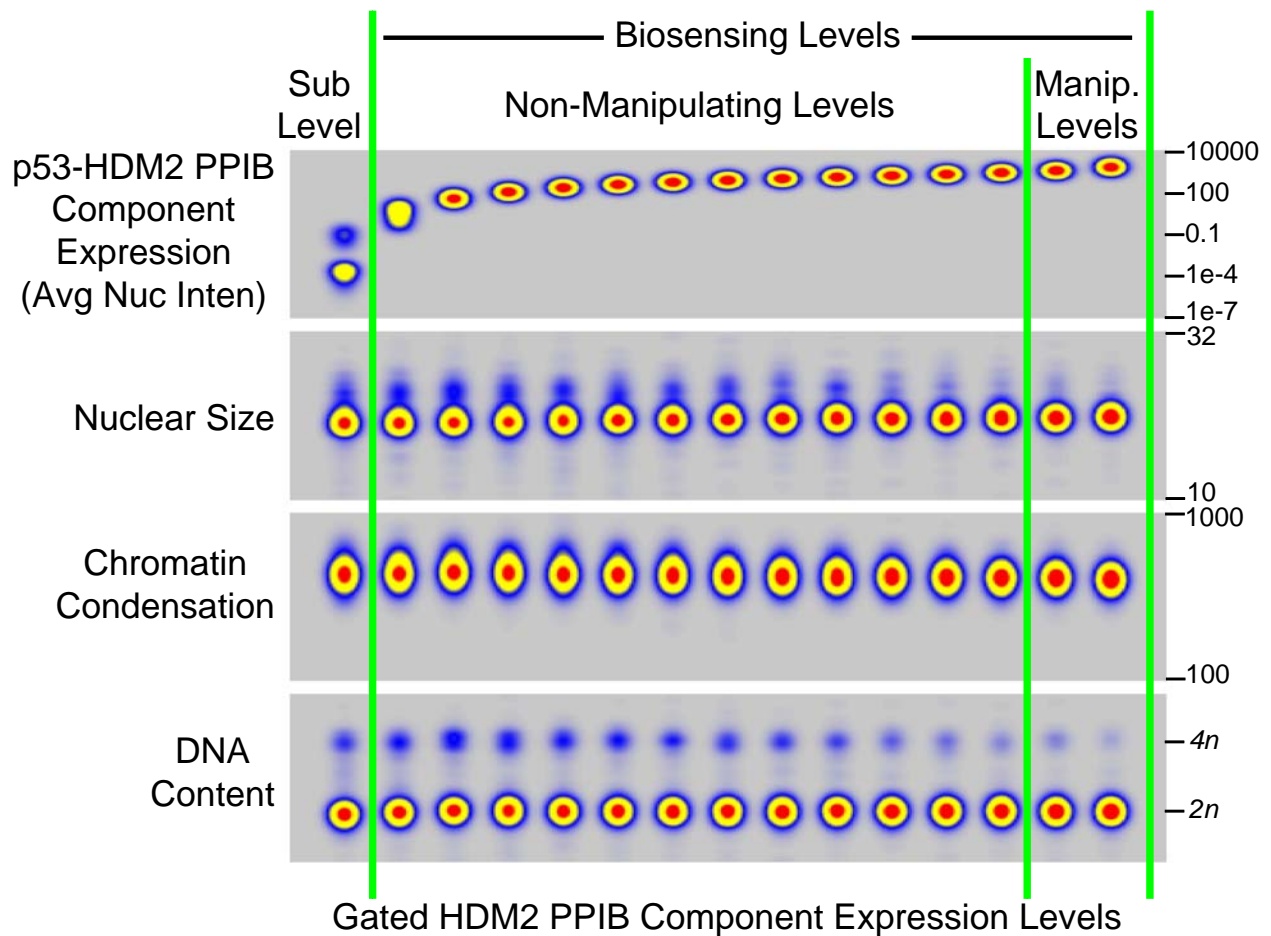


Figure 2. Gating biosensor expression levels produced large populations of biosensing cells with non-perturbing levels of the p53-HDM2 PPIB. A549 cells were infected with a combination of two adenoviruses encoding the PPIB components (p53:HDM2 component ratio of 40:1) for only 24 h. Distribution maps show multiple cell population responses for cell cycle and nuclear morphology (Y-axis). Populations of cells were binned according to their expression level of the HDM2 PPIB component (X-axis). The top map shows the cell population distribution of PPIB expression levels in each of the 15 bins. The other maps show biomarker feature measurements of key cell activity for cells in each of the PPIB expression bins. Under these conditions of

adenoviral infection, the population of cells in which no PPIB expression could be detected was < 10% of the total population (*Sub Level*). In the cells where PPIB expression was detected (*Biosensing Levels*), 80% of the population expressed the PPIB at a level that did not perturb the cells (*Non-Manipulating Levels*). Gating the signal levels of the PPIB therefore resulted in a large population of non-perturbed cells that were qualified for inclusion in a CSB profiling model of disease.

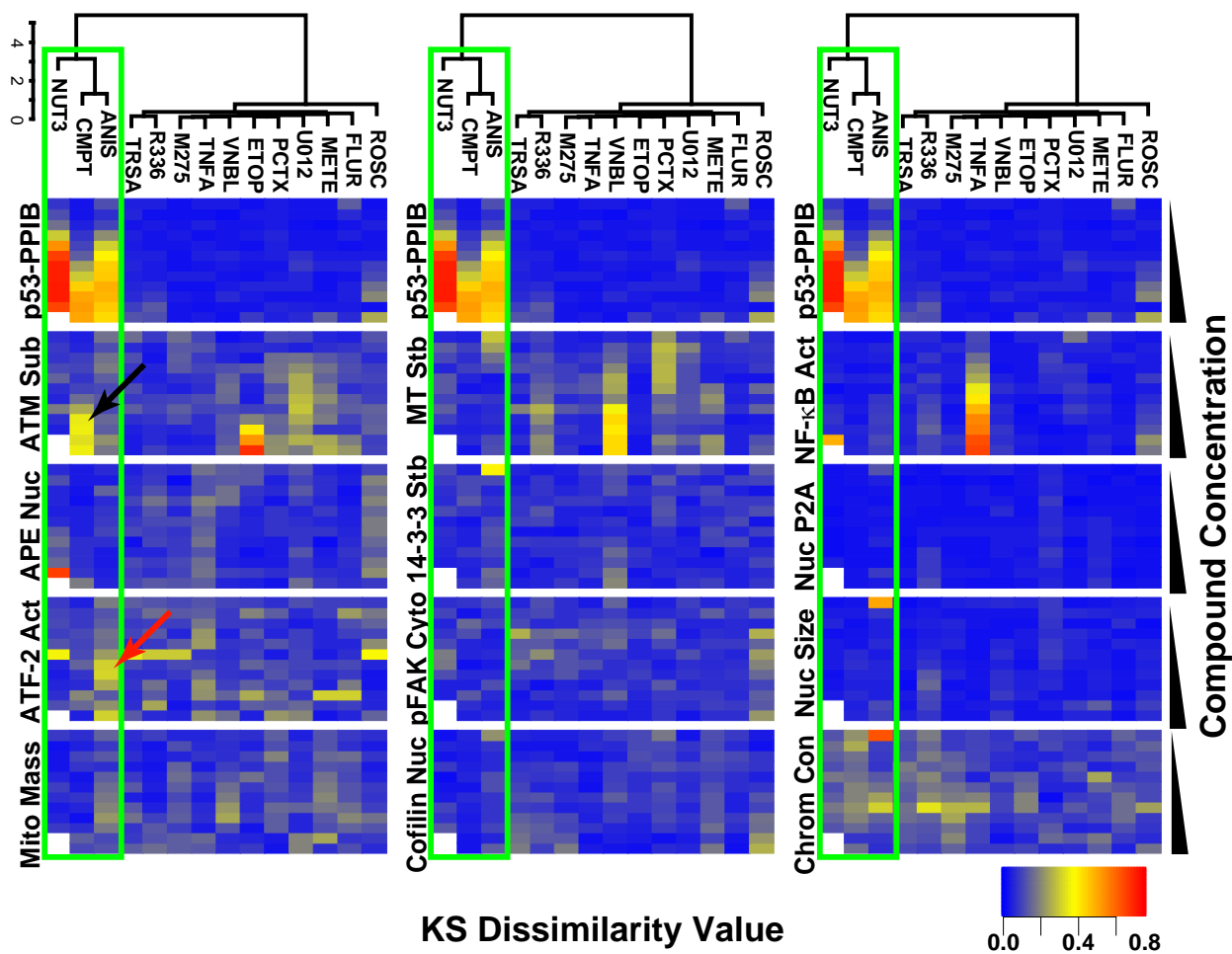


Figure 3. Cluster analysis of a large CSB profiling database provided automated high-level information on the cellular systems response to modulators of the p53-HDM2 interaction. A549 cells expressing the p53-HDM2 PPIB at qualified biosensing levels were treated with a set of 14 compounds known to exhibit a wide range of activities (see Table 1). After a 2 h incubation, cells were fixed and 12 biomarker activities were measured (See Table 2) in addition to the activity of the p53-HDM2 PPIB to produce a CSB response profile. The compounds were clustered according to their ability to modulated the p53-HDM2 interaction. These heat maps were produced using KS dissimilarity measurements that compared the responses of untreated cell populations with cell populations treated with compounds [10, 11]. The clustering results for p53-HDM2 PPIB activity were applied to each of the other biomarker measurements. To

facilitate the visual inspection of the large set of heat maps, the heat map and corresponding dendrogram for the PPIB response was repeated at the top of each column of heat maps. For example, the cluster enclosed in the green boxes contained the compounds with the greatest p53-HDM2 interaction modulating activity, nutlin-3, camptothecin, and anisomycin. Reading down each heat map in the same column enabled comparisons to be made about the effects that each compound had on the multiple cellular systems profiled. In this example, where the primary screening target was modulation of the p53-HDM2 interaction, both camptothecin and anisomycin had significant off-target effects, which may lead to a toxic response at longer treatment times. For example, camptothecin also induced a significant change in the activity of ATM kinase at several concentrations (black arrow) and anisomycin also significantly modulated the phosphorylation level of the stress kinase substrate transcription factor ATF-2 (red arrow).

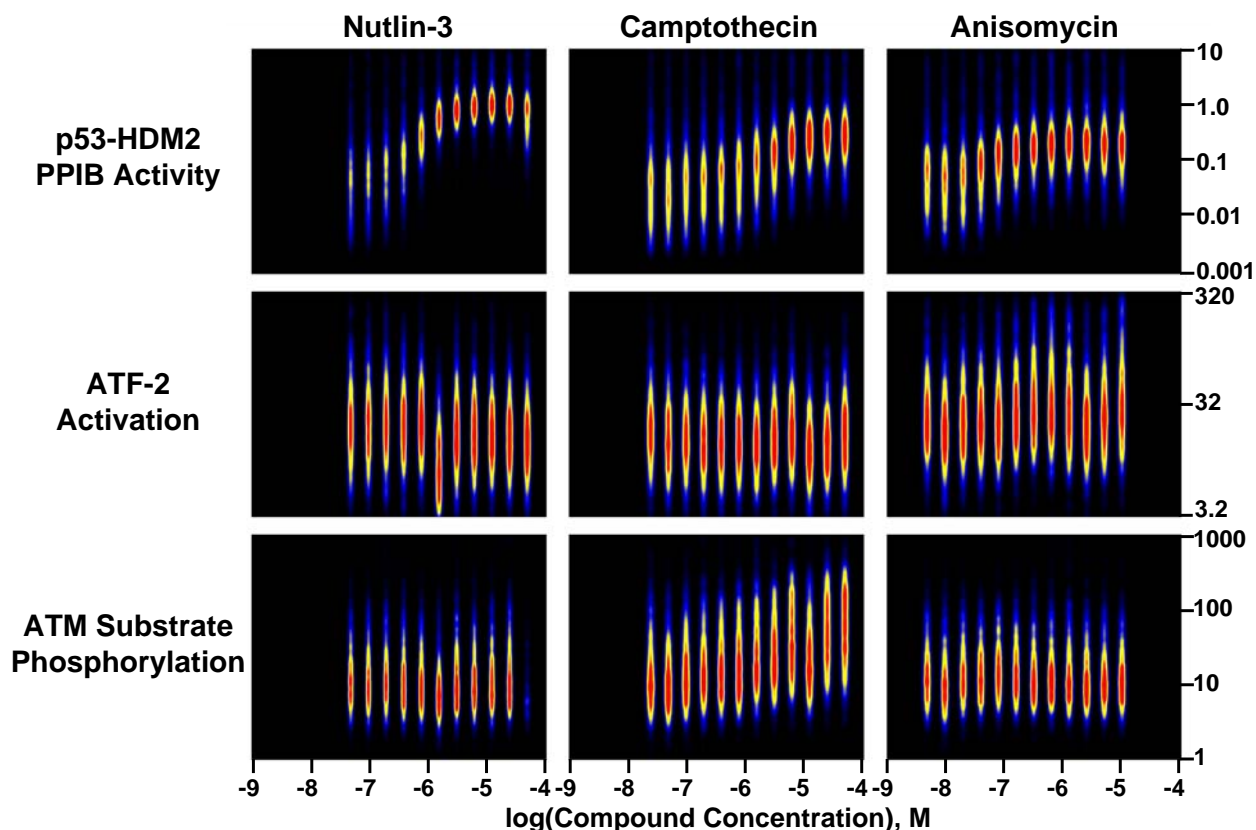


Figure 4. Drilling down into the mechanisms of action of p53-HDM2 interaction disrupting compounds. Distribution Maps were used to visualize the cell population responses to the three p53-HDM2 interaction modulators defined in the initial CSB profiling analysis (Figure 3). These maps show the cellular population response at each compound concentration using a color coded density map. The cooler blue colors represent low cell densities and the warmer yellow and red colors represent the highest cell densities. The top row of maps show that nutlin-3 was not only the most active compound in disrupting the p53-HDM2 interaction ( $AC_{50} = 1 \mu\text{M}$ ), but that it induced a more homogeneous cellular population response than did either camptothecin or anisomycin, consistent with nutlin-3 exhibiting a higher degree of specificity for the p53-HDM2 interaction. Furthermore, nutlin-3 induced minimal activation of ATF-2 or increased levels of ATM kinase substrate phosphorylation, consistent with a target specificity greater than camptothecin or anisomycin, which significantly modulated ATF-2 activity and ATM kinase

substrate phosphorylation, respectively. These results suggest that nutlin-3 directly modulates the p53-HDM2 interaction, which it is designed to do, and that camptothecin and anisomycin disrupt p53-HDM2 over the same time course by activating indirect regulatory pathways.

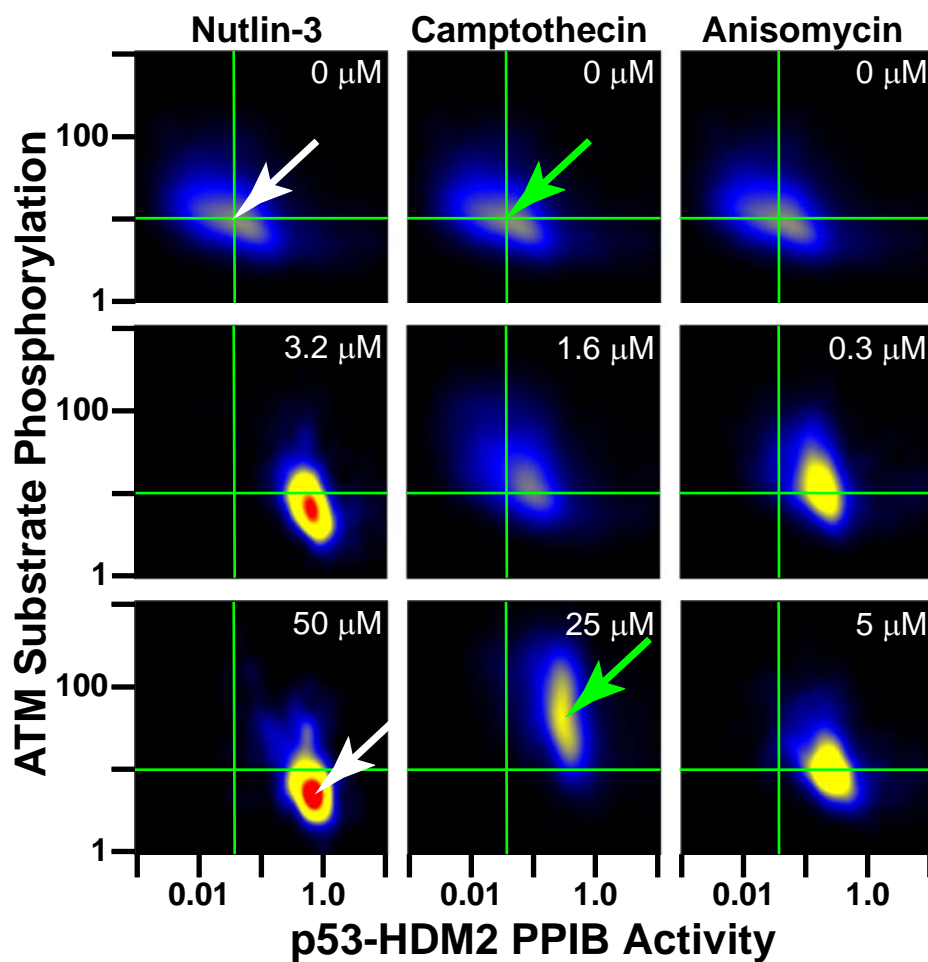


Figure 5. Cellular systems biology profiling can be used to classify compound activities based on the relationships between the cellular biomarkers they modulate. Cell maps were used to show the effects three compounds had on the relationships between two functional biomarkers and use the same color coding scheme described for the Distribution maps. The activity of the p53-HDM2 biosensor (X-axis) was plotted against the level of ATM kinase substrate phosphorylation in the same population of cells treated with nutlin-3, camptothecin, or anisomycin at concentrations selected from the distribution maps shown in Figure 4. The green fiduciary lines, which facilitate comparisons between graphs, are the same in each map and are centered on the population distribution of the untreated cells.

For nutlin-3, which had the greatest p53-HDM2 interaction disrupting activity out of the compound set we tested, the homogeneous increase in biosensor activity was indicated by a horizontal right shift as well as increased population density (compare locations of the two white arrows). Nutlin-3 exhibited maximal disruption of the p53-HDM2 interaction over the treatment range of 3.2  $\mu\text{M}$  to 50  $\mu\text{M}$ . Nutlin-3 also induced a small decrease (*e.g.*, downward vertical shift) in the ATM kinase substrate phosphorylation level was also seen to occur in the same cell population that exhibited maximal p53-HDM2 interaction disruption. On the other hand, camptothecin, at half the concentration of nutlin-3, induced a heterogeneous increase in ATM kinase substrate phosphorylation levels in the same cell population that it caused a moderate disruption of the p53-HDM2 interaction (compare locations of the two green arrows). Anisomycin maximally disrupted the p53-HDM2 interaction at concentrations between 0.3 and 10  $\mu\text{M}$ , but was nearly an order of magnitude less efficacious than nutlin-3. Nevertheless, anisomycin, like nutlin-3, showed p53-HDM2 interaction disrupting activity without increasing or decreasing the ATM kinase substrate phosphorylation levels in the same cell population.

## References

1. Verneti, L.; Irwin, W.; Giuliano, K. A.; Gough, A.; Johnston, K.; Taylor, D. L., Cellular systems biology applied to pre-clinical safety testing: A case study of CellCiphr™ profiling. In *Drug efficacy, safety, and biologics discovery: Emerging technologies and tools*, Xu, J. J.; Ekins, S., Eds. Wiley & Sons: New Jersey, 2008; p (in press).
2. Critchley-Thorne, R. J.; Miller, S. M.; Lingle, W. L.; Taylor, D. L., Applications of cellular systems biology in breast cancer patient stratification and diagnostics. *Combinatorial Chemistry and High Throughput Screening: Thematic issue on in vitro imaging* **2008**, (in press).
3. Taylor, D. L.; Giuliano, K. A., Multiplexed high content screening assays create a systems cell biology approach to drug discovery. *Drug Discovery Today: Technologies* **2005**, 2, (2), 149-154.
4. Giuliano, K. A.; Johnston, P. A.; Gough, A.; Taylor, D. L., Systems cell biology based on high-content screening. *Methods Enzymol* **2006**, 414, 601-19.
5. Taylor, D. L., Haskins, J.R., and Giuliano, K.A., *High Content Screening: A Powerful Approach to Systems Cell Biology and Drug Discovery*. Humana Press: Totowa, NJ, 2006; Vol. 356, p 444.
6. Taylor, D. L., Insights into High Content Screening: Past, Present and Future. In *High Content Screening: A Powerful Approach to Systems Cell Biology and Drug Discovery*, Taylor, D. L., Haskins, J.R., and Giuliano, K.A., Ed. Humana Press: Totowa, NJ, 2006; pp 3-18.
7. Giuliano, K. A.; Premkumar, D.; Taylor, D. L., Optimal characteristics of protein-protein interaction biosensors for cellular systems biology profiling. In *High Content Screening: Science, Technology, and Applications*, Haney, S. A., Ed. Wiley: New York, 2007; p (in press).
8. Giuliano, K. A.; Taylor, D. L.; Waggoner, A. S., Reagents to measure and manipulate cell functions. In *High Content Screening: A Powerful Approach to Systems Cell Biology and Drug Discovery*, Taylor, D. L., Haskins, J.R., and Giuliano, K.A., Ed. Humana Press: Totowa, NJ, 2006; Vol. 356, pp 141-163.
9. Mizuguchi, H.; Kay, M. A., Efficient construction of a recombinant adenovirus vector by an improved in vitro ligation method. *Hum Gene Ther* **1998**, 9, (17), 2577-83.
10. Giuliano, K. A.; Cheung, W. S.; Curran, D. P.; Day, B. W.; Kassick, A. J.; Lazo, J. S.; Nelson, S. G.; Shin, Y.; Taylor, D. L., Systems cell biology knowledge created from high content screening. *Assay Drug Dev Technol* **2005**, 3, (5), 501-14.
11. Giuliano, K. A.; Chen, Y. T.; Taylor, D. L., High-content screening with siRNA optimizes a cell biological approach to drug discovery: Defining the role of p53 activation in the cellular response to anticancer drugs. *J. Biomol. Screening* **2004**, 9, (7), 557-568.
12. Thompson, T.; Tovar, C.; Yang, H.; Carvajal, D.; Vu, B. T.; Xu, Q.; Wahl, G. M.; Heimbrook, D. C.; Vassilev, L. T., Phosphorylation of p53 on key serines is dispensable for transcriptional activation and apoptosis. *J Biol Chem* **2004**.
13. Schon, O.; Friedler, A.; Bycroft, M.; Freund, S.; Fersht, A., Molecular Mechanism of the Interaction between MDM2 and p53. *J Mol Biol* **2002**, 323, (3), 491-501.
14. Vassilev, L. T.; Vu, B. T.; Graves, B.; Carvajal, D.; Podlaski, F.; Filipovic, Z.; Kong, N.; Kammlott, U.; Lukacs, C.; Klein, C.; Fotouhi, N.; Liu, E. A., In vivo activation of the p53 pathway by small-molecule antagonists of MDM2. *Science* **2004**, 303, (5659), 844-8.
15. Thompson, T.; Tovar, C.; Yang, H.; Carvajal, D.; Vu, B. T.; Xu, Q.; Wahl, G. M.; Heimbrook, D. C.; Vassilev, L. T., Phosphorylation of p53 on Key Serines Is Dispensable for Transcriptional Activation and Apoptosis. *J Biol Chem* **2004**, 279, (51), 53015-22.

16. Collins, F. S.; Green, E. D.; Guttmacher, A. E.; Guyer, M. S., A vision for the future of genomics research. *Nature* **2003**, 422, (6934), 835-47.
17. Collins, F. S.; Morgan, M.; Patrinos, A., The human genome project: lessons from large-scale biology. *Science* **2003**, 300, (5617), 286-90.
18. Phillips, K. A.; Van Bebber, S. L., Measuring the value of pharmacogenomics. *Nat Rev Drug Discov* **2005**, 4, (6), 500-9.
19. Costa, F. F., Non-coding RNAs: new players in eukaryotic biology. *Gene* **2005**, 357, (2), 83-94.
20. Cummins, J. M.; He, Y.; Leary, R. J.; Pagliarini, R.; Diaz, L. A., Jr.; Sjoblom, T.; Barad, O.; Bentwich, Z.; Szafarska, A. E.; Labourier, E.; Raymond, C. K.; Roberts, B. S.; Juhl, H.; Kinzler, K. W.; Vogelstein, B.; Velculescu, V. E., The colorectal microRNAome. *Proc Natl Acad Sci USA* **2006**, 103, (10), 3687-92.
21. Huttenhofer, A.; Schattner, P.; Polacek, N., Non-coding RNAs: hope or hype? *Trends Genet* **2005**, 21, (5), 289-97.
22. Volinia, S.; Calin, G. A.; Liu, C. G.; Ambs, S.; Cimmino, A.; Petrocca, F.; Visone, R.; Iorio, M.; Roldo, C.; Ferracin, M.; Prueitt, R. L.; Yanaihara, N.; Lanza, G.; Scarpa, A.; Vecchione, A.; Negrini, M.; Harris, C. C.; Croce, C. M., A microRNA expression signature of human solid tumors defines cancer gene targets. *Proc Natl Acad Sci USA* **2006**, 103, (7), 2257-61.
23. Melnick, J. S.; Janes, J.; Kim, S.; Chang, J. Y.; Sipes, D. G.; Gunderson, D.; Jarnes, L.; Matzen, J. T.; Garcia, M. E.; Hood, T. L.; Beigi, R.; Xia, G.; Harig, R. A.; Asatryan, H.; Yan, S. F.; Zhou, Y.; Gu, X. J.; Saadat, A.; Zhou, V.; King, F. J.; Shaw, C. M.; Su, A. I.; Downs, R.; Gray, N. S.; Schultz, P. G.; Warmuth, M.; Caldwell, J. S., An efficient rapid system for profiling the cellular activities of molecular libraries. *Proc Natl Acad Sci USA* **2006**, 103, (9), 3153-8.
24. Hopkins, A. L.; Groom, C. R., Opinion: The druggable genome. *Nat Rev Drug Discov* **2002**, 1, (9), 727-30.
25. Yang, Y.; Blomme, E. A.; Waring, J. F., Toxicogenomics in drug discovery: from preclinical studies to clinical trials. *Chem Biol Interact* **2004**, 150, (1), 71-85.
26. Glocker, M. O.; Guthke, R.; Kekow, J.; Thiesen, H. J., Rheumatoid arthritis, a complex multifactorial disease: on the way toward individualized medicine. *Med Res Rev* **2006**, 26, (1), 63-87.
27. Jain, S.; Wood, N. W.; Healy, D. G., Molecular genetic pathways in Parkinson's disease: a review. *Clin Sci (Lond)* **2005**, 109, (4), 355-64.
28. Nadeau, J. H.; Burrage, L. C.; Restivo, J.; Pao, Y. H.; Churchill, G.; Hoit, B. D., Pleiotropy, homeostasis, and functional networks based on assays of cardiovascular traits in genetically randomized populations. *Genome Res* **2003**, 13, (9), 2082-91.
29. Tuomisto, T. T.; Binder, B. R.; Yla-Herttuala, S., Genetics, genomics and proteomics in atherosclerosis research. *Ann Med* **2005**, 37, (5), 323-32.